COMPENSATION OF DISTURBANCES ON SELF-SENSING MAGNETIC BEARINGS CAUSED BY SATURATION AND COORDINATE COUPLING

Norbert Skricka and **Richard Markert**
Department of Applied Mechanics, Darmstadt University of Technology
Hochschulstr. 1, D-64289 Darmstadt, Germany
markert@mechanik.tu-darmstadt.de, skricka@mechanik.tu-darmstadt.de

ABSTRACT

Self-sensing is a posibility to simplify active magnetic bearing systems. In this paper a method to determine the rotor position in magnetic bearings by measuring the clock-frequent components of the coil current and voltage generated by pulse width modulated amplifiers is discussed. Ways are pointed out to overcome the problems resulting from the ambiguity of the identification signals due to the non-linearities of the magnets as well as to avoid the distortions of the identification signals due to magnetic coupling between the individual magnets.

INTRODUCTION

Today, most magnetic bearing systems are assembled of separate components (controller, power amplifiers, electromagnets, sensors, signal conditioning). They have some inherent disadvantages, like high sensitiveness, high maintenance expenditure, expensive production and limited capacity, which considerably hinder a general acceptance and greater dissemination, [2,3]. These disadvantages of conventionally assembled magnetic bearing systems can be reduced significantly by functional and structural integration, [4]. Self-sensing is one of various potentialities to achieve this goal. Instead of measuring the actual rotor position by separate contactless displacement sensors, the rotor position is identified from the current and voltage signals of the magnetic bearing coils, [5,7].

PRINCIPLE OF SELF-SENSING

Figure 1 shows the principle of an electromagnetic bearing. Current i and voltage u applied to a coil of an electromagnetic bearing are linked by the resistance R_M of the coil and the inductance L_M of the electromagnet,

$$\frac{d}{dt}\left(L_M\, i\right) + R_M\, i = u\,. \tag{1}$$

Therefore the inductance L_M can basically determined from the measured electrical signals u and i. The inductance L_M of the electromagnet changes with the rotor position z, which enables to estimate the rotor position by inverting the relation between the inductance and the air gap.

In systems with pules-width-modulated power amplifiers the current i and the voltage u are composed of low-frequency and high frequency components, whereas the rotor motion does not contain high frequency parts as a consequence of its inertia. The clock frequency (for example 40 kHz) is very

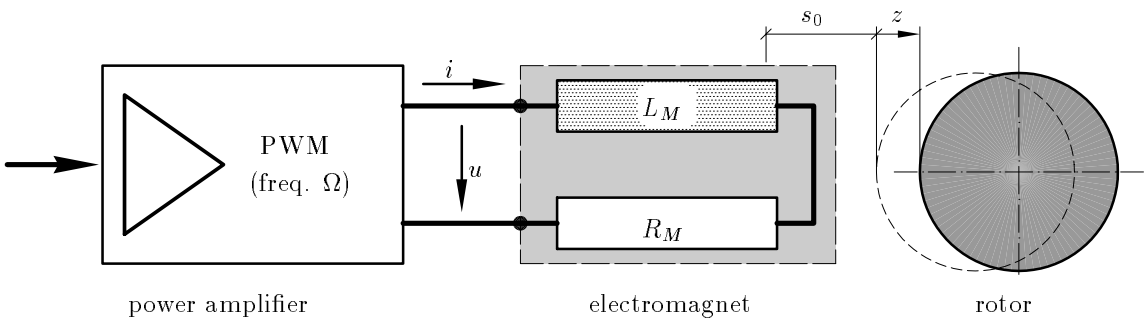

FIGURE 1: Principle of a self-sensing bearing

high compared to the frequencies of the mechanical rotor vibrations. In this sence the state variables are given by

$$\begin{aligned} i &= i_0(t) + \hat{i}_\Omega(t)\, e^{j\Omega t}, \\ u &= u_0(t) + \hat{u}_\Omega(t)\, e^{j\Omega t} \quad \text{and} \\ z &= z_0(t), \end{aligned} \tag{2}$$

neglecting higher harmonics of the clock frequency $f_\Omega = \Omega/2\pi$. In other words, the low-frequency components $i_0(t)$ and $u_0(t)$ are varying slowly with time and are responsible for levitating and moving the rotor, whereas the high frequency components of the electrical signals do not affect the mechanical behavior.

The developed selfsensing method for determining the rotor position z uses the clock-frequent components of the electrical signals. Only the amplitudes $\hat{u}_\Omega$ and $\hat{i}_\Omega$ have to be measured. This is done by extracting the high frequency components from the total electrical signals, rectifying and averaging them.

The measured amplitudes of the electrical signals are composed to a single measurement quantity

$$v_M = 2\, k_M\, \Omega \left| \frac{\hat{i}_\Omega}{\hat{u}_\Omega} \right|, \tag{3}$$

which is a non-linear measure for the actual air gap $s = s_0 + z$ between the magnet and the rotor. The design parameters of the electromagnets are taken into account by the constant

$$k_M = \frac{n^2 \mu_L A_L \cos\alpha}{4}. \tag{4}$$

Due to the magnetic saturation of the core material the inductance L_M is not as in the ideal case independent of the current i and inverse proportional to the air gap $s = s_0 + z$. On the contrary, it depends in complicated manner on the air gap and on the current, $L_M = L_M(s, i)$. Therefore the inductance can not be represented by an analytic formula in general case.

Considering the fact, that the inductance depends on the current and on the air gap, equation (1) will get the following form,

$$L_M \frac{di}{dt} + \frac{\partial L_M}{\partial i} \frac{di}{dt}\, i + \frac{\partial L_M}{\partial s}\, \dot{z} + R\, i = u. \tag{5}$$

Frequency-selective analysis of this relationship shows, that the clock-frequent components of the two last terms on the left side of equation (5) are small compared to the others and can be neglected. This results from the facts that
a) the resistance R_M of the coil is usually small (for example 0.22 Ohm) compared to the reactance $\Omega\, L_M$ (for example 1 k Ohm) and
b) the rotor velocity $\dot{z}$ does not contain high frequency vibrations. Therefore the measurement quantity v_M and the inductance L_M are related by

$$v_M = \frac{2k_M}{L_M + \dfrac{\partial L_M}{\partial i} i_0}. \tag{6}$$

MAGNETS WITHOUT SATURATION

Before dealing with real magnets, the principle for estimating the rotor position from the clock-frequent electrical signals will be explained on the basis of the ideal case. Neglecting the saturation the inductance is inversely proportional to the air gap and independent of the current,

$$L_M = \frac{2k_M}{s_0 + z}. \tag{7}$$

Therefore in this ideal case equation (6) simplifies to

$$v_M = s_0 + z, \tag{8}$$

thus the rotor position z depends linearly on the measurement quantity v_M.

NON-LINEARITIES OF THE MAGNETS

Due to saturation of real magnets, the inductance L_M is determined by the magnetic permeability of the core material, witch depends non-linearly on the magnetic field $\boldsymbol{H}$. The magnetic field is generated by the current density $\boldsymbol{J}$ in the coils fulfilling the equation $\mathrm{rot}\, \boldsymbol{H} = \boldsymbol{J}$. The magnetic flux density $\boldsymbol{B}$ depends non-linearly on the magnetic field $\boldsymbol{H}$ due to the fact, that the permeability of the core material changes with the magnetic field, $\mu(|\boldsymbol{H}|)$.

Taking into account the saturation, the inductance L_M is computed by equating the magnetic energy described by $\boldsymbol{B}$ and $\boldsymbol{H}$ on one hand,

$$W_M = \frac{1}{2} \int_V \boldsymbol{B} \cdot \boldsymbol{H}\, dV, \tag{9}$$

to that one described by L_M and i on the other hand,

$$W_M = \frac{1}{2}\, L_M\, i^2. \tag{10}$$

The total magnetic energy W_M includes the energy stored in the core, the air gap and also the air around the magnet. Comparing the two representations of the magnetic energy W_M the real inductance

$$L_M(s, i) = \frac{\int_V \boldsymbol{B} \cdot \boldsymbol{H}\, dV}{i^2} \tag{11}$$

becomes a non-linear function of the air gap $s = s_0 + z$ and the coil current i. It can be calculated by FEM programs for every given coil current and air gap, [6]. Figure 3 shows the computed inductance $L_M(s,i)$ of the electromagnet sketched in figure 2. The air gap varies from 0.025 mm to 0.9 mm and the coil current from 0.25 A to 5.0 A. The ideal inductance of the electromagnet neglecting the saturation effect is shown in figure 3 as bold line.

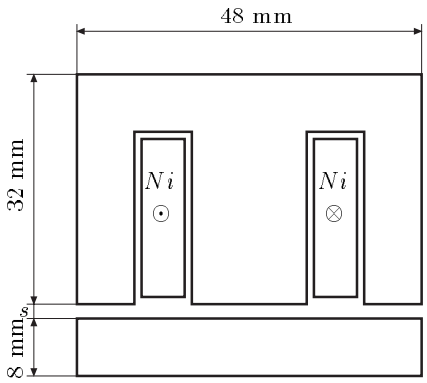

FIGURE 2: Geometry of the example magnet for computing the inductance $L_M(s_0+z,i)$, coil: 95 windings, core material: EBG 110-35

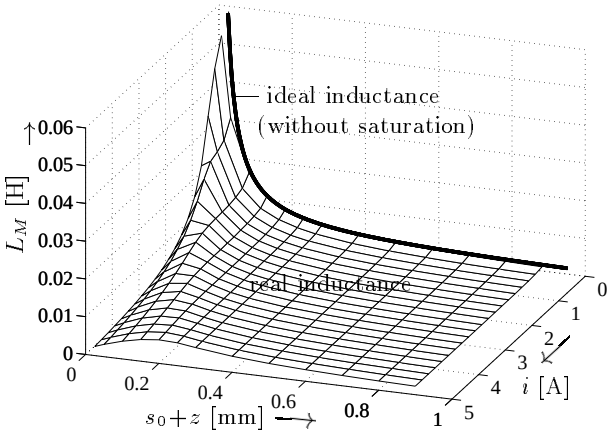

FIGURE 3: Computed real inductance $L_M(s,i)$ of the electromagnet shown in figure 2 (taking into account saturation) compared to the ideal inductance (neglecting saturation)

For small coil currents the computed real inductance fits the ideal one described by equation (7). But for large coil currents and small air gaps the real inductance is clearly smaller than the ideal one.

Figure 4 shows the scaled inverse inductance $2k_M/L_M$ as a function of the air gap $s = s_0 + z$ and the coil current i. As can be seen the scaled inverse inductance $2k_M/L_M$ is a measure for the rotor position z.

In the ideal case the measurement quantity v_M is

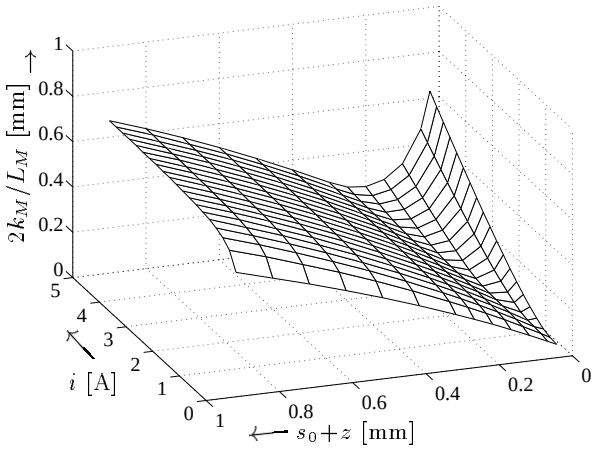

FIGURE 4: Scaled inverse inductance

identical with the air gap $s = s_0 + z$. But due to saturation and scattering leakage there is a big difference between the measurement quantity v_M and the non-linear inverse inductance $2k_M/L_M$. And beyond it the air gap is not unambiguously assignable to the scaled inverse inductance.

NON-LINEAR MEASURING

Equation (6) describes the non-linear relation between the measurement quantity v_M and the inductance $L_M(s,i)$. The inductance depents on the air gap as shown in figure 3. Based on equation (1) these non-linear behavior of an electromagnet was investigated numerically using MATLAB/SIMULINK. The power amplifier was described by a PWM and the signals $\widehat{i}_\Omega$ and $\widehat{u}_\Omega$ were extracted from the total signals by bandpass filters like in the experiments. Figure 5 shows the measurement quantity $v_M = 2k_M\Omega|\widehat{i}_\Omega/\widehat{u}_\Omega|$ resulting from the simulations.

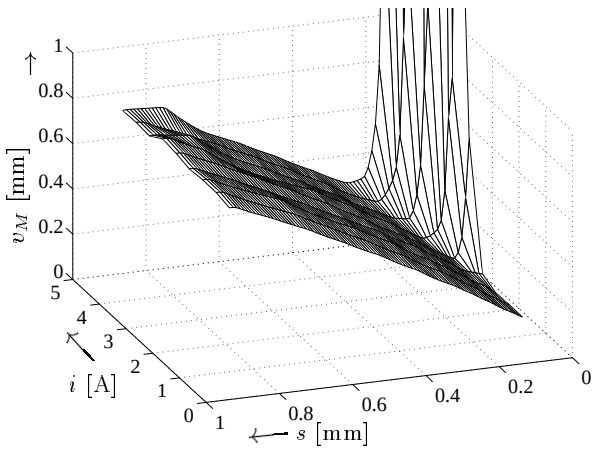

FIGURE 5: Measurement quantity $v_M = 2k_M\Omega|\widehat{i}_\Omega/\widehat{u}_\Omega|$ resulting from simulations

Compared to figure 4 the measurement quantity rises much steeper within the area of magnetic saturation.

This results from the term $\partial L_M/\partial i \cdot i_0$ in equation (6), which has to be added to the inductance L_M shown in figure 4.

Figure 6 shows the identified measurement quantity $v_M = 2k_M\Omega|\widehat{i}_\Omega/\widehat{u}_\Omega|$ measured on a real magnetic system. The experimental system used corresponds to that one of the simulation. The measured results are very close to the simulated ones. It must be noted that the smallest air gap in the measurement is 0.1 mm and therefore the strong non-linear effects are not as obvious as in figure 5. The differences between measured and simulated quantity v_M result from the eddy current effects and leakage flux in the third dimension which were neglected by the 2-dimensional FEM simulation.

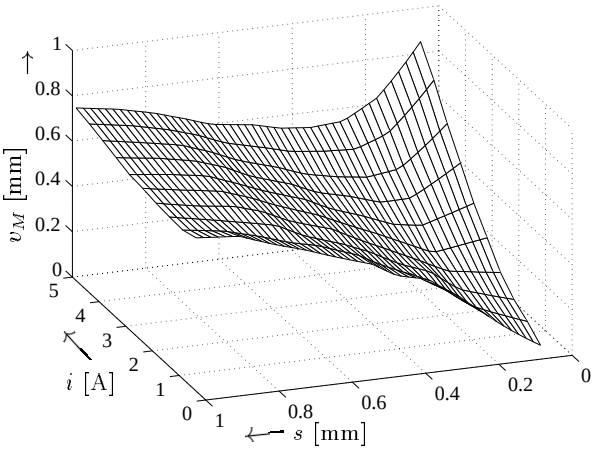

FIGURE 6: Measurement quantity $v_M = 2k_M\Omega|\widehat{i}_\Omega/\widehat{u}_\Omega|$ measured on a real electromagnet

IDENTIFICATION WITH TWO MAGNETS

Due to the magnetic saturation, the relation between the measurement quantity v_M and the rotor position z is ambiguous. But in most magnetic bearings two opposite magnets are used for levitating one direction. Using both opposite magnets simultaniously the rotor position can be determined correct.

In figure 7 the relation between the rotor position z and the corresponding values v_+ and v_- for the identification quantities resulting from the two opposite electromagnets with different coil currents are shown.

In general for each magnet two values for the rotor position can be found in the characteristic curve, z_{1v_+}, z_{2v_+} from the z_+ magnet and z_{1v_-} and z_{2v_-} from the z_- magnet as shown in figure 7. Two of them are close together indicating the correct rotor position. In the shown example the values z_{2v_+} and z_{2v_-} are indicating the correct rotor position z. The

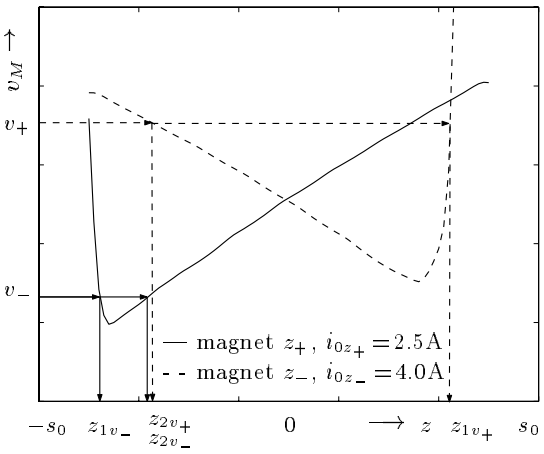

FIGURE 7: Finding the correct rotor position from the measured quantities v_- and v_+

possible values for the rotor position z can be found by scanning the characteristic of the measurement quantity v_M (figure 6) for the measured value with respect to the coil current. In practice this is a very slow and laborious technique. It is easier to invert the characteristic diagram for v_M concerning to the rotor position. Due to the ambiguity it is necessary to divide the characteristic diagram into two strictly monotonous areas and inverting each separately.

The described analysis can carried out by software in the digital controller, e.g. on a DSP or a FPGA, [1].

COORDINATE COUPLING OF THE BEARING MAGNETS

In figure 8 the magnetic field (equipotential lines of the magnetic vector potential) in the bearing estimated by FEM simulations is shown. The rotor is located at $z = -0.3$ mm and the coil currents of the four electromagnets are different. The coupling effect can be seen by field lines connecting two electromagnets. Couplings occur between neighboured magnets as well as between opposite magnets, which depend in a complex way on the coil currents and the rotor position. In practice these magnetic couplings makes the accuracy of the rotor position estimated from electrical signals worse.

The coupling effects can be suppressed by modified bearing constructions, e.g. by separating the individual electromagnets by air gaps in the stator metal. This reduces the magnetic coupling as can be seen by comparing figure 9 and figure 8. The coil currents and rotor position are the same in the two figures. As expected, there is no magnetic flux over the stator back, but there is still a remarkable magnetic coupling over the rotor.

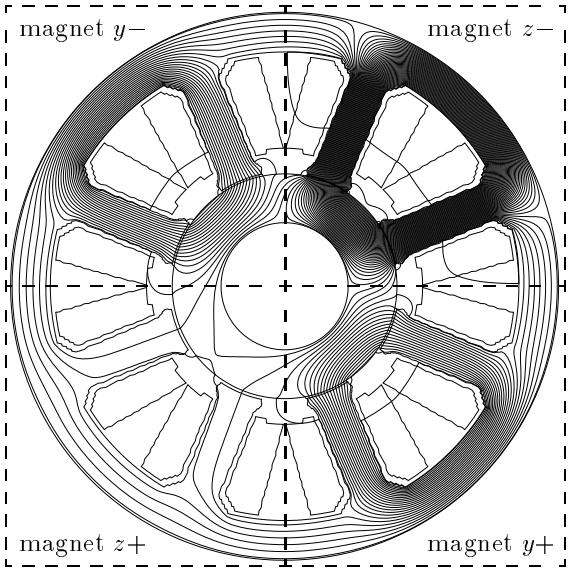

FIGURE 8: Magnetic field lines in the bearing with closed stator for coil currents $i_{z+} = 0.5$A, $i_{z-} = 5.0$A, $i_{y+} = 2.25$A, $i_{y-} = 2.25$A and rotor position $z = 0.3$ mm, $y = 0$

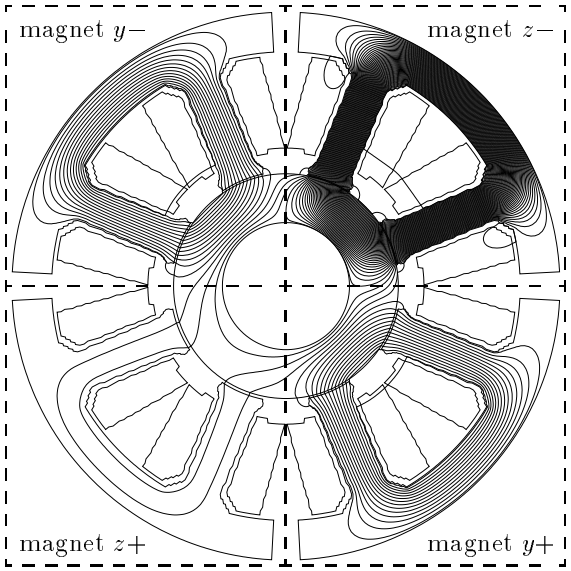

FIGURE 9: Magnetic field lines with air gaps in the stator for coil currents $i_{z+} = 0.5$A, $i_{z-} = 5.0$A, $i_{y+} = 2.25$A, $i_{y-} = 2.25$A and rotor position $z = 0.3$ mm, $y = 0$

Another way to avoid magnetic coupling can be realized by short circuit wires winded around the back of the stator between the magnets instead of air gaps. The AC-parts of the magnetic field induce currents in the wires. These currents generate a magnetic field, which works contrarily to the causing field. But it does't work against the DC-part of the magnetic field, which carries the rotor.

Electromagnets with three poles can also reduce the problem resulting from magnetic coupling. By the order of the magnetic poles the magnets guard themselves against each other. The magnetic fields of an individual magnet is independent from the other electromagnets. But it must be pointed out that a higher number of magnet poles in the bearing leads to lager losses during rotation due to the change of the magnetization.

ACKNOWLEDGEMENTS

This research project is supported by the Deutsche Forschungsgemeinschaft within the SFB 241.

REFERENCES

1. Glesner M., T. Le, M.-D. Doan, A. Kirschbaum, F.-M. Renner: On the Methodology and Design of Application Specific Processors for Mechatronic Systems. Proc. of the 4th Int. Workshop on Mixed Design of Integrated Circuits and Systems, Poznan, Poland (1997), pp. 41 – 54.

2. Hoffmann, K.-J., R. Markert: Linearisierung von magnetischen Lagerungen für elastische Rotoren per Software (Linearization of Magnetic Bearings for Elastic Rotors by Software). Mechatronik im Maschinen- und Fahrzeugbau, VDI-Berichte 1315 (1997), pp. 407 – 418.

3. Hoffmann, K.-J.: Integrierte aktive Magnetlager (Integrated Active Magnetic Bearings). Diss. TU Darmstadt, CGA-Verlag, Reihe Mechatronik (1999)

4. Isermann, R.: Mechatronische Systeme (Mechatronic Systems). Automatisierungstechnik 43 (1995) 12, Oldenbourg, pp. 540 – 548.

5. Laier, D.: Nichtlinearitäten magnetgelagerter Rotorsysteme (Non-linearities of Magnetically Suspended Rotor Systems). Diss. TU Darmstadt, Fortschritt-Berichte VDI, Reihe 11, Nr. 273 (1999).

6. Profi Engineering Systems GmbH: User manual program system PROFI, Darmstadt (1997)

7. Vischer, D.: Sensorlose und spannungsgesteuerte Magnetlager (Sensorless and Voltage Controlled Magnetic Bearings). Diss. ETH Zürich, Nr. 8665 (1988).